

Exploring bisphenol S removal mechanism with multi-enzymes extracted from waste sludge and reed sediment

Guangying Hou

Shandong University

Zaihui Huang (✉ 912278608@qq.com)

Shandong University

Xiaohu Ding

Weifang Ecological Environmental Protection Bureau

chunguang liu

Shandong University

Research Article

Keywords: Bisphenol, Enzymolysis, Bio-flocculation, Waste sludge, Reed sediment

Posted Date: May 5th, 2022

DOI: <https://doi.org/10.21203/rs.3.rs-1442986/v1>

License:   This work is licensed under a Creative Commons Attribution 4.0 International License.

[Read Full License](#)

Abstract

BPS, as a widespread environmental hormone-like micro-pollutants, is difficult to be degraded in the environment. In this study, the removal of BPS with multi-enzymes extracted from waste sludge and reed sediment were studied at 25°C, 37°C and 55°C. Results show that BPS could be removed efficiently, which could involve enzymolysis and bio-flocculation. The mechanism and pathways of the enzymolysis were identified with LC-MS/MS. Polymerization of BPS with enzymolysis further improved the removal by bio-flocculation due to the production of BPS oligomers. Furthermore, the interaction mechanism between BPS and multi-enzymes was explored through a series of spectroscopic experiments. Results show that more loose skeletal structure of the multi-enzymes and more hydrophobic microenvironment of the amino acid residues are responsible for the removal of BPS. This research not only provided a method for refractory micropollutants removal but also a way for the utilization of waste sludge and reed sediment.

1. Introduction

More and more evidences about the toxic effects of 4,4'-Isopropylidenediphenol (BPA) were reported (Bernardo et al. 2021, Tišler et al. 2016). In order to meet the restrictions and regulations, manufacturers are gradually using 4,4'-sulfonyl-diphenol (BPS) instead of BPA as a substitute for industrial applications (Cai & Zhang 2022). However, studies have shown that BPS also possesses geno-toxicity and estrogenic activity similar to that of BPA (Chen et al. 2002, Grignard et al. 2012). Another study from Japan suggests that BPS appears to be more resistant to environmental degradation than BPA (Ike et al. 2006, Silva et al. 2012), which made it more hazardous. In addition, the occurrence of BPS in all types of environmental matrices was reported (Viñas et al. 2010). For example, BPS in sewage sludge was up to 523 mg/kg dw (Lee et al. 2015, Song et al. 2014), which resulted in the release of BPS into rivers due to improper processing, from where even into groundwater, drinking water, and soil, adversely affecting environmental ecosystems and human health (Garcia-Rodríguez et al. 2014, Wang et al. 2015).

Many articles reported various methods for the removal of BPS, including advanced oxidation (Repousi et al. 2017), adsorption (Banihashemi & Droste 2014), flocculation and biological degradation (Fudala-Ksiazek et al. 2018, Liu et al. 2016, Sasaki et al. 2005). However, these methods also showed shortcomings such as high cost, secondary pollution, time-consuming and so on. Among these ways, biological degradation is a better alternative. However, current wastewater treatment plants aim to remove phosphorus, nitrogen and bio-degradable organic matter through the metabolic activity of a variety of microbial communities (Krah et al. 2016, Reis et al. 2017), but exhibits low efficiency and long lag time to the organics micro-pollutants (e.g. BPS). On the other hand, sewage sludge contains many kinds of enzymes (including intracellular and extracellular enzymes) which can degrade micropollutants at high efficiency (Braun et al. 2011, Villemur et al. 2013). Endophytic bacteria from rhizomes and roots of reed plants were widely used for micropollutant degradation and bioremediation, owing to their extracellular enzymes which serve either a protective function and oxidise extracellular toxic soluble phenolic metabolites to insoluble polymerized products, or a degradative function and oxidise polymeric lignin or phenols for metabolic purposes (Harvey et al. 2002, He et al. 2017, Sauvêtre et al. 2018). Daniel

Krah et al. used native extracellular enzymes extracted from waste sludge to remove pharmaceuticals, biocides and personal care products (Krah et al. 2016), but the relative removal mechanism was not clarified enough. Intracellular enzymes could also inevitably show a high metabolic versatility in the degradation of micro-contaminants (Fischer & Majewsky 2014, Sasaki et al. 2005). However, few reports focus on the removal of bisphenol chemicals (e.g. BPS) from aqueous solution with the intracellular and extracellular enzymes extracted from sludge and reed sediment. It has been reported that the use of multi-enzyme complexes can significantly promote the overall degradation efficiency of substrates (Huang et al. 2019). Thus, it is meaningful to study the BPS removal with multi-enzymes and the interaction mechanism. In addition, physiological structure of the multi-enzymes affects its lifetime, which is a key factor the utilization of enzymes (Odnell et al. 2016). While several studies showed that BPS not only could induce DNA damage (Grelska & Noszczyńska 2020), but also irreversibly bind serum albumin, pepsin, trypsin and α -amylase, resulting in the change of physiological structure and function the enzymes and an increased risk of metabolic syndrome (Rezg et al. 2019, Usman & Ahmad 2016, Yang et al. 2016). Therefore, it is necessary to explore the change of physiological structure and function of multi-enzymes induced by BPS in the process of BPS removal.

The aims of this study are to (i) provide a new method for BPS removal in aqueous solution with the multi-enzymes from waste sludge and reveal the removal mechanism, (ii) to clarify the effect of the structure and function of the multi-enzymes on BPS removal.

2. Material And Methods

2.1 Chemicals

Biphenol S was purchased from Aladdin Industrial Corporation (Shanghai, China). Sodium chloride, sodium hydroxide, disodium hydrogen phosphate and sodium dihydrogen phosphate are of analytical grade. HEPES-buffer (50 mmol/L HEPES, 50 mmol/L NaCl, pH 7.4) was used for the extraction of enzymes from sludge and reed sediment. Phosphate buffer (0.2 mol/L, pH = 7.4, contain 0.1 mol/L NaCl) was also used during the interaction process between BPS and multi-enzymes. BPS (250 mg/L) was dissolved with ultrapure water.

2.2 Procedure of the experiments

2.2.1 Sampling & processing of waste sludge

Chemical oxygen demand (COD) and pH of the waste sludge are 30000 mg/L and 6.8. The sludge was stored in a refrigerator at 4°C after collecting from a secondary sedimentation tank (daily flow rate: 300000 m³, hydraulic retention time: 12 h, sludge retention time: 12 d) of Jinan Everbright Water Treatment Plant. Reed sediment were obtained from Baiyun Lake in Jinan, Shandong Province. Firstly, the reed sediment was well mixed with water. Then 100 ml of the sludge and reed sediment were centrifuged for 6 min at 5000 rpm in a swing-bucket rotor, respectively. The supernatant was then discarded and 10 ml of HEPES-buffer (50 mmol/L HEPES, 50 mmol/L NaCl, pH 7.4) was added. Subsequently, the sample

was homogenized on a vortex homogenizer for 2 min. Finally, the quasi-homogeneous sludge and reed sediment were well mixed for the extraction of multi-enzymes.

2.2.2 Extraction of multi-enzymes

Extraction method reported in the literature (Krah et al. 2016) was used in this research with modification, shown as follows. The sample was placed in an ice-water bath and sonicated with a sonication micro-tip (sonics materials inc CV188 connected to Sonics Vibra-Cell™ (VCX150PB) at 10 mm immersion depth in a 50 mL tube. The parameters for ultrasonication were power (20 KHz), energy (100 Watts) and time (10 minutes). In order to avoid sample being heated, sonication was conducted at an interval of 15 s with 15 s breaks. After ultrasonication, the sample was centrifuged for 20 min at 14000 rpm to remove cell debris, and the crude cell lysate (supernatant) was then filtered through 0.45 µm polyethersulfone (PES) membrane to remove residual cells. The filtrate was kept at ice-water bath.

2.2.3 Characteristics of multi-enzymes

COD was determined with standard methods to characterize the concentration of the multi-enzymes (Federation W E 2005). Content of DNA in the multi-enzymes was determined with micro-amount method with spectrophotometer (ND-2000, Nanodrop) to analysis the degree of cell disruption. Protein content was measured with coomassie brilliant blue method. The kit was bought from Nanjing Jiancheng Bioengineering Institute. Assays were incubated for 10min and absorbance was measured at 545 nm. The protein concentration was calculated by the following equation:

$$C(g/L) = \frac{A_{sample} - A_{blank}}{A_{standard} - A_{blank}} \times 0.563g/L$$

1

Three-dimensional excitation-emission-matrix (EEM) fluorescence spectrometry (F-4600, Hitachi, Japan) with software MatLab 7.0 and sodium dodecyl sulfate polyacrylamide gel electrophoresis (SDS-PAGE) were used to characterize the main protein component and the molecular weight of the multi-enzymes.

2.3 Removal of BPS with multi-enzymes

In order to understand the mechanism of BPS removal, blank control group, negative control group and experimental groups were set. Multi-enzymes (2 mL), PBS buffer (pH 7.4, 1 ml) and BPS (0.8 mL) were added to a series of 10 mL colorimetric tubes, then diluted to 10 mL with ultrapure water. Among them, the multi-enzymes of negative control group was treated with high temperature (10 min incubation at 100°C) to inactive the enzymes. For the blank control group, BPS was instead by ultrapure water. For the experimental groups, effect of temperature on the degradation of BPS was studied by setting the reaction temperature at 25°C, 37°C and 55°C. The reaction continued 60 h with sampling at 5 time points (1 h, 8 h, 24 h, 48 h and 60 h). All samples were prepared in triplicate. The content of BPS were determined with a ultra-high performance liquid chroma-tograph (UPLC, Thermo Ultimate 3000 high performance liquid chromatograph, United States) connected to an API 3200 (Sciex, Concord, Canada) triple stage quadrupole mass spectrometer with electrospray ionization (ESI). The LC-MS/MS conditions were set and

calibrated according to a reference (Kolatorova Sosvorova et al. 2017) with some modification as follows. Before detection, multi-enzymes was removed with ultrafilter (Millipore amicon ultra-30/10K). The mobile phase consisted of methanol and water (ratio of 9:1). Column temperature, analysis time and flow rate was 50°C, 12 min and 0.4 ml/min, respectively.

2.4 Interaction of BPS and multi-enzymes

In order to explore the removal mechanism of BPS by the multi-enzymes, UV-vis, fluorescence and resonance fluorescence were used to clarify the interaction between multi-enzymes and BPS with different concentration.

2.4.1 UV-vis absorption spectra analysis

To explore the conformation change of multi-enzymes, UV-vis absorption spectra were measured with a UV-2450 spectrophotometer (Shimadzu, Japan) at the wavelength range of 190–350 nm. The concentration of multi-enzymes was kept constant, while the concentration of BPS varied from 0 to 20 mg/L. All the samples were analyzed after reaction for half an hour.

2.4.2 Fluorescence spectra analysis

To further clear the interaction mechanism, fluorescence spectra were performed in a fluorescence spectrophotometer (F-4600, Hitachi, Japan) with a wavelength range of 290–420 nm. The measured excitation wavelength, photo multiplier tube voltage, slit width and scanning speed were set as 280 nm, 650 V, 5 nm and 1200 nm/min, respectively. Synchronous fluorescence spectra were obtained under a fixed wavelength interval ($\Delta\lambda = 15$ nm and $\Delta\lambda = 60$ nm) between excitation and emission wavelength. The other operation parameters were same as those of fluorescence. Fluorescence quenching mechanism was determined according to Stern-Volmer equation, shown as follows.

$$F_0/F = 1 + K_{SV}[Q] = 1 + k_q\tau_0[Q] \quad (2)$$

Where F and F_0 present the fluorescence intensities with and without quencher, respectively. K_{SV} , $[Q]$, k_q and τ_0 was the Stern-Volmer quenching constant, concentration of the quencher, quenching rate constant of the biological macromolecule and fluorescence lifetime without quencher. For the biological macromolecule, the maximum dynamic quenching constant of various quenchers is 2.0×10^{10} mol/l/s (Ware 1962).

3. Results And Discussion

3.1 Evaluation of multi-enzymes from sludge

EEM was used to characterize the multi-enzymes, due to the association between peaks and tyrosine-like, tryptophan-like, humic-like, or phenol-like organic compounds (Chen et al. 2003). Generally, five regions

can be divided (shown in Fig. 1A). Regions I and II (EX < 250 nm, EM < 350 nm) involve in simple aromatic proteins such as tyrosine. Region III (EX < 250 nm, EM > 350 nm) involves fulvic acid-like materials. Region IV (EX = 250–280 nm, EM < 380 nm) involve soluble microbial byproduct-like and tryptophan-like material. Region V (EX > 280 nm, EM > 380 nm) is involved in humic acid-like organics. As shown in Fig. 1A, multi-enzymes were comprised with simple aromatic proteins and soluble microbial byproduct-like materials. SDS-PAGE followed by zymogram analysis suggest that the molecular weights of the multi-enzymes contained several enzymes. The molecular weight were about 60, 44, 22.3 and 13.7 kDa, respectively (Fig. 1B). Combined with the degradation products of bisphenol S (shown in part 3.2) and literature about laccase (Sauvêtre et al. 2018, Zdarta et al. 2018), it can be inferred that the complex enzyme may contain laccase. Besides proteins in the multi-enzymes, little DNA are also contented (shown in Table 1).

Table 1
Characteristics of the multi-enzymes.

Item	COD (mg/L)	Protein (mg/L)	DNA (mg/L)
Multi-enzymes	660.6	370.8	50.9

3.2 Removal of BPS by multi-enzymes

As shown in Fig. 2, the concentration of BPS decreases over time at 25°C, 37°C and 55°C. Highest removal rate (89.1%) was obtained after the reaction for 60 h at 55°C. Before the formation of flocs (first 48 h), lower reaction temperature (25°C and 310K) shows higher removal rate (43.8% and 51.4%) than that of 33.3% at higher reaction temperature (55°C). The reaction system with highest temperature of 55°C first produced flocs at about 38th h. Flocs observed at 49th h and 53th h in the reaction systems with the temperature of 310K and 25°C, respectively. The removal rate of BPS sharply increases with white flocs on the rise. Therefore, no less than two removal mechanisms exist in this reaction process, which could involve enzymolysis and bio-flocculation. Single removal mechanism have been certified. For example, Krah et al. (2016) extracted multi-enzymes for micropollutants removal by enzymolysis. By comparing the removal rates of BPS at different time and temperatures, a conclusion could be drawn that enzymolysis pre-dominants the removal of BPS before the formation of flocs, which also were affected by the reaction temperature. The optimum temperature for multi-enzymes activity could be at or near 37°C.

In order to further certificate the role of enzymolysis, a negative control test was set. In the control test, the multi-enzymes was inactivated by heating at 100°C for 10 min. Results showed that the removal rate of BPS (about 4.3%) was less than that of active multi-enzymes (about 43.8%, 51.4% and 33.3%) before 48th h, which indicates enzymolysis plays an important role for the removal of BPS. Although flocs also observed at 36th h, inactivation did not boost the production of flocs. The amount of flocs was not higher than that of un-inactivated multi-enzymes in experimental groups. After filtration, part of the flocs re-dissolved with ultra-pure water by ultrasound treatment for determination of the COD, protein content and DNA. The characteristics of the flocs in the reaction system were further analyzed. As shown in Table 2,

the amount of flocs (COD concentration) is the largest in the reaction system with highest temperature of 55°C, followed by that 310K and 298K. Compared to the initial multi-enzymes, the content of protein in the flocs obviously increased. The remaining parts of flocs were enriched with acetonitrile extraction to determine the content with LC-MS/MS. LC-MS/MS analysis data of the main transformation products are listed in Table 3 and Fig.S1. The m/z values with the largest relative abundance were 498 and 746, respectively, which corresponded to the molecular weights of dimer BPS and trimer BPS, respectively. Formation of two kinds of BPS oligomers suggested the multi-enzymes enhanced the bio-transform with polymerization way (Catherine et al. 2016, Majeau et al. 2010). Hydroxylated BPS (m/z = 266) were identified which indicated some bio-transformation of BPS involved in other way (e.g. p450 way (Skledar et al. 2016)). Based on the intermediate products identified here, a schematic view of the pathways for BPS degradation by multi-enzymes was proposed (Fig. 3). Polymerization of BPS enhanced the removal of BPS by bio-flocculation.

Table 2
Characteristics of the flocs from the reaction system.

Item	328 K	310 K	298 K
COD (mg/L)	220.80	175.30	96.50
Protein (mg/L)	54.63	39.56	29.82
Content of BPS (mg/L)	8.62	4.33	2.67

Table 3
Characterization of main BPS bio-transformation products detected by means of LC- MS/MS.

R _t (min)	Pseudo-Molecular ion formula	m/z [M-H] ⁻	Δ(ppm)
10.5	C ₁₂ H ₁₀ O ₄ S	249.2701 (BPS)	2.5
11.3	C ₁₂ H ₁₀ O ₅ S	265.1026	1.6
18.5	C ₂₄ H ₁₈ O ₈ S	497.403	1.3
23.6	C ₃₆ H ₂₆ O ₁₂ S	745.3052	2.7

3.3 Interaction mechanism

From the results of experimental group and control test, one conclusion could be drawn that the inactivation of the multi-enzymes leads to the decrease for removal of BPS, not only in the enzymolysis stage, but also in bio-flocculation stage. Therefore, it is important to clarify the mechanism of inactivation of multienzyme.

3.3.1 Effect of BPS on the skeleton structure of the multi-enzymes

UV spectroscopy is a simple method for detecting protein structural change. The enzyme possesses two main absorption peaks, one of which is a strong absorption peak around 210 nm, representing the protein skeleton. The other weak absorption peak is around 280 nm, which can reflect the change of amino acid residue microenvironment (Zhang et al. 2008). The UV-vis absorption spectra of multi-enzymes with BPS exposure are shown in Fig. 4. The absorption peak height of multi-enzymes increases little, as the addition dosage is lower, but decreased obviously with the increase of BPS addition, accompanying by red shift. The phenomenon suggested the $\pi \rightarrow \pi^*$ electronic transitions of multi-enzymes and the loosening and unfolding of the multi-enzymes skeleton (Hao et al. 2015).

3.3.2 Fluorescence spectral analysis

As shown in Fig. 5A and 5B, intrinsic fluorescence could be emitted with the excitation at 280 nm, which is attributed to the multi-enzymes contained tryptophan and tyrosine. The fluorescence intensity decreased depending on the concentration of BPS with blue shift, which illuminated that BPS quenched the fluorescence of multi-enzymes (Lakowicz 2008). According to Stern-Volmer equation, the value of K_{sv} decreased with the increase of reaction temperature from 37°C to 55°C (shown in Fig. 6). In addition the value of K_q is much larger than $2 \times 10^{10} \text{ L}\cdot\text{mol}^{-1}\cdot\text{s}^{-1}$. Therefore, the quenching mechanism could be static quench.

3.3.3 Synchronous Fluorescence

Synchronous fluorescence was performed to assess tyrosine ($\Delta\lambda = 15 \text{ nm}$) and tryptophan ($\Delta\lambda = 60 \text{ nm}$) residues microenvironment changes (Wang et al. 2008). As shown in Fig. 7A and 7B, with the increase of BPS concentration, the fluorescence intensity of the multi-enzymes significantly decreased with an obvious red shift, which illustrated that BPS caused the microenvironment of tyrosine residues become more hydrophobic (Klajnert & Bryszewska 2002). On the other hand, Fig. 7C and 7D shows that the fluorescence intensity displayed gradual lower inward with the increase of BPS addition without red or blue shift, suggesting that BPS changes the microenvironment of tryptophan (Lu et al. 2011). Compared with the synchronous fluorescence between $\Delta\lambda = 15 \text{ nm}$ and $\Delta\lambda = 60 \text{ nm}$, BPS is more likely to cause the conformational change around tyrosine residues.

3.4 Visualized description of BPS removal by multi-enzymes

Removal mechanism of BPS is shown in Fig. 8. Enzymolysis and flocculation are involved in BPS removal. Simultaneously, BPS and multi-enzymes interacted in the removal process, which resulted in a more loose skeleton structure of multi-enzymes and a more hydrophobic microenvironment of tryptophan and tyrosine residues. This change could further affect the activity of multi-enzymes as well as BPS removal both in enzymolysis and bio-flocculation process.

4. Conclusion

BPS can be efficiently removed by the multi-enzymes extracted from waste sludge and reed sediment. Removal mechanisms involved enzymolysis and bio-flocculation, which were all bound up with the activity of multi-enzymes. Enzymolysis predominated BPS removal before the production of flocs, but bio-flocculation played a key role for BPS removal with the formation of flocs. In addition, reaction temperature showed important effect on BPS removal and the removal mechanisms. Spectroscopic analysis indicated that, with the addition of BPS, microenvironment of amino acid (tryptophan and tyrosine) residues and skeleton structure of multi-enzymes became more hydrophobic and more loose, which were responsible for the activity change of multi-enzymes and BPS removal both in enzymolysis and bio-flocculation process.

Declarations

Funding: This study has been supported by Shandong Provincial Natural Science Foundation, China (ZR2019BB049).

Data availability: The datasets used and/or analyzed during the current study are available from the corresponding author on reasonable request.

Author contribution: Guangying Hou: writing original draft, data curation, investigation, methodology; Zaihui Huang: investigation, writing original draft, formal analysis; Chunguang Liu: experiment design, data analysis, and writing.

Competing Interests: The authors have no competing interests to declare that are relevant to the content of this article.

Ethical Approval and Consent: All the authors agreed to submit and publish the paper and stated that this study did not involve ethical issues.

References

1. Banihashemi B, Droste RL (2014) Sorption–desorption and biosorption of bisphenol A, triclosan, and 17 α -ethinylestradiol to sewage sludge. *Sci Total Environ* 487:813–821
2. Bernardo RA, Sousa JCP, Gallimberti M, Junior FB, Vaz BG, Chaves AR (2021) A fast and direct determination of bisphenol S in thermal paper samples using paper spray ionization mass spectrometry. *Environ Sci Pollut Res Int* 28:57288–57296
3. Braun F, Hamelin J, Gévaudan G, Patureau D (2011) Development and application of an enzymatic and cell flotation treatment for the recovery of viable microbial cells from environmental matrices such as anaerobic sludge. *Appl Environ Microbiol* 77:8487–8493
4. Cai J, Zhang Y (2022) Enhanced degradation of bisphenol S by persulfate activated with sulfide-modified nanoscale zero-valent iron. *Environ Sci Pollut Res Int* 29:8281–8293

5. Catherine H, Penninckx M, Frédéric D (2016) Product formation from phenolic compounds removal by laccases: A review. *Environ Technol Innov* 5:250–266
6. Chen M-Y, Ike M, Fujita M (2002) Acute toxicity, mutagenicity, and estrogenicity of bisphenol-A and other bisphenols. *Environ Toxicol* 17:80–86
7. Chen W, Westerhoff P, Leenheer JA, Booksh K (2003) Fluorescence Excitation – Emission Matrix Regional Integration to Quantify Spectra for Dissolved Organic Matter. *Environ Sci Technol* 37:5701–5710
8. Federation W, E APHA (2005) : Standard methods for the examination of water and wastewater.. American Public Health Association (APHA): Washington, DC, USA
9. Fischer K, Majewsky M (2014) Cometabolic degradation of organic wastewater micropollutants by activated sludge and sludge-inherent microorganisms. *Appl Microbiol Biotechnol* 98:6583–6597
10. Fudala-Ksiazek S, Pierpaoli M, Luczkiewicz A (2018) Efficiency of landfill leachate treatment in a MBR/UF system combined with NF, with a special focus on phthalates and bisphenol A removal. *Waste Manag* 78:94–103
11. Garcia-Rodríguez A, Matamoros V, Fontàs C, Salvadó V (2014) The ability of biologically based wastewater treatment systems to remove emerging organic contaminants—a review. *Environ Sci Pollut Res* 21:11708–11728
12. Grelska A, Noszczyńska M (2020) White rot fungi can be a promising tool for removal of bisphenol A, bisphenol S, and nonylphenol from wastewater. *Environ Sci Pollut Res Int* 27:39958–39976
13. Grignard E, Lapenna S, Bremer S (2012) Weak estrogenic transcriptional activities of Bisphenol A and Bisphenol S. *Toxicol In Vitro* 26:727–731
14. Hao F, Jing M, Zhao X, Liu R (2015) Spectroscopy, calorimetry and molecular simulation studies on the interaction of catalase with copper ion. *J Photochem Photobiol B* 143:100–106
15. Harvey PJ, Campanella BF, Castro PML, Harms H, Lichtfouse E, Schäffner AR, Smrcek S, Werck-Reichhart D (2002) Phytoremediation of polyaromatic hydrocarbons, anilines and phenols. *Environ Sci Pollut Res* 9:29–47
16. He Y, Langenhoff AAM, Sutton NB, Rijnaarts HHM, Blokland MH, Chen F, Huber C, Schröder P (2017) Metabolism of Ibuprofen by *Phragmites australis*: Uptake and Phytodegradation. *Environ Sci Technol* 51:4576–4584
17. Huang Y, Li J, Yang Y, Yuan H, Wei Q, Liu X, Zhao Y, Ni C (2019) Characterization of enzyme-immobilized catalytic support and its exploitation for the degradation of methoxychlor in simulated polluted soils. *Environ Sci Pollut Res Int* 26:28328–28340
18. Ike M, Chen MY, Danzl E, Sei K, Fujita M (2006) Biodegradation of a variety of bisphenols under aerobic and anaerobic conditions. *Water Sci Technol* 53:153–159
19. Klajnert B, Bryszewska M (2002) Fluorescence studies on PAMAM dendrimers interactions with bovine serum albumin. *Bioelectrochemistry* 55:33–35

20. Kolatorova Sosvorova L, Chlupacova T, Vitku J, Vlk M, Heracek J, Starka L, Saman D, Simkova M, Hampl R (2017) Determination of selected bisphenols, parabens and estrogens in human plasma using LC-MS/MS. *Talanta* 174:21–28
21. Krah D, Ghattas A-K, Wick A, Bröder K, Ternes TA (2016) Micropollutant degradation via extracted native enzymes from activated sludge. *Water Res* 95:348–360
22. Lakowicz JR (2008) Principles of fluorescence spectroscopy | Clc. *J Biomed Opt* 13:029901
23. Lee S, Liao C, Song G-J, Ra K, Kannan K, Moon H-B (2015) Emission of bisphenol analogues including bisphenol A and bisphenol F from wastewater treatment plants in Korea. *Chemosphere* 119:1000–1006
24. Liu N, Liang G, Dong X, Qi X, Kim J, Piao Y (2016) Stabilized magnetic enzyme aggregates on graphene oxide for high performance phenol and bisphenol A removal. *Chem Eng J* 306:1026–1034
25. Lu D, Zhao X, Zhao Y, Zhang B, Zhang B, Geng M, Liu R (2011) Binding of Sudan II and Sudan IV to bovine serum albumin: Comparison studies. *Food Chem Toxicol* 49:3158–3164
26. Majeau J-A, Brar SK, Tyagi RD (2010) Laccases for removal of recalcitrant and emerging pollutants. *Bioresour Technol* 101:2331–2350
27. Odnell A, Recktenwald M, Stensén K, Jonsson B-H, Karlsson M (2016) Activity, life time and effect of hydrolytic enzymes for enhanced biogas production from sludge anaerobic digestion. *Water Res* 103:462–471
28. Reis BG, Silveira AL, Tostes Teixeira LP, Okuma AA, Lange LC, Amaral MCS (2017) Organic compounds removal and toxicity reduction of landfill leachate by commercial bakers' yeast and conventional bacteria based membrane bioreactor integrated with nanofiltration. *Waste Manag* 70:170–180
29. Repousi V, Petala A, Frontistis Z, Antonopoulou M, Konstantinou I, Kondarides DI, Mantzavinos D (2017) Photocatalytic degradation of bisphenol A over Rh/TiO₂ suspensions in different water matrices. *Catal Today* 284:59–66
30. Rezg R, Abot A, Mornagui B, Knauf C (2019) Bisphenol S exposure affects gene expression related to intestinal glucose absorption and glucose metabolism in mice. *Environ Sci Pollut Res Int* 26:3636–3642
31. Sasaki M, Akahira A, Oshiman K-i, Tsuchido T, Matsumura Y (2005) Purification of Cytochrome P450 and Ferredoxin, Involved in Bisphenol A Degradation, from *Sphingomonas* sp. Strain A01. *Appl Environ Microbiol* 71:8024–8030
32. Sauvêtre A, May R, Harpaintner R, Poschenrieder C, Schröder P (2018) Metabolism of carbamazepine in plant roots and endophytic rhizobacteria isolated from *Phragmites australis*. *J Hazard Mater* 342:85–95
33. Silva CP, Otero M, Esteves V (2012) Processes for the elimination of estrogenic steroid hormones from water: A review. *Environ Pollut* 165:38–58
34. Skledar DG, Schmidt J, Fic A, Klopčič I, Trontelj J, Dolenc MS, Finel M, Mašič LP (2016) Influence of metabolism on endocrine activities of bisphenol S. *Chemosphere* 157:152–159

35. Song S, Song M, Zeng L, Wang T, Liu R, Ruan T, Jiang G (2014) Occurrence and profiles of bisphenol analogues in municipal sewage sludge in China. *Environ Pollut* 186:14–19
36. Tišler T, Krel A, Gerželj U, Erjavec B, Dolenc MS, Pintar A (2016) Hazard identification and risk characterization of bisphenols A, F and AF to aquatic organisms. *Environ Pollut* 212:472–479
37. Usman A, Ahmad M (2016) : From BPA to its analogues: Is it a safe journey? *Chemosphere* 158, 131–142
38. Villemur R, dos Santos SCC, Ouellette J, Juteau P, Lépine F, Déziel E (2013) Biodegradation of Endocrine Disruptors in Solid-Liquid Two-Phase Partitioning Systems by Enrichment Cultures. *Appl Environ Microbiol* 79:4701–4711
39. Viñas P, Campillo N, Martínez-Castillo N, Hernández-Córdoba M (2010) Comparison of two derivatization-based methods for solid-phase microextraction–gas chromatography–mass spectrometric determination of bisphenol A, bisphenol S and biphenol migrated from food cans. *Anal Bioanal Chem* 397:115–125
40. Wang J, Wang X, Xiong C, Liu J, Hu B, Zheng L (2015) Chronic bisphenol A exposure alters behaviors of zebrafish (*Danio rerio*). *Environ Pollut* 206:275–281
41. Wang T, Xiang B, Wang Y, Chen C, Dong Y, Fang H, Wang M (2008) Spectroscopic investigation on the binding of bioactive pyridazinone derivative to human serum albumin and molecular modeling. *Colloids Surf B* 65:113–119
42. Ware WR (1962) Oxygen quenching of fluorescence in solution: an experimental study of the diffusion process. *J Phys Chem* 66:455–458
43. Yang H, Hou G, Zhang L, Ju L, Liu C (2016) Exploring the effect of bisphenol S on sludge hydrolysis and mechanism of the interaction between bisphenol S and α -Amylase through spectrophotometric methods. *Biology, Journal of Photochemistry and Photobiology B*
44. Zdarta J, Antecká K, Frankowski R, Zgoła-Grześkowiak A, Ehrlich H, Jesionowski T (2018) The effect of operational parameters on the biodegradation of bisphenols by *Trametes versicolor* laccase immobilized on *Hippospongia communis* spongin scaffolds. *Sci Total Environ* 615:784–795
45. Zhang YZ, Chen XX, Dai J, Zhang XP, Liu YX, Liu Y (2008) Spectroscopic studies on the interaction of lanthanum(III) 2-oxo-propionic acid salicyloyl hydrazone complex with bovine serum albumin. *Luminescence* 23:150

Figures

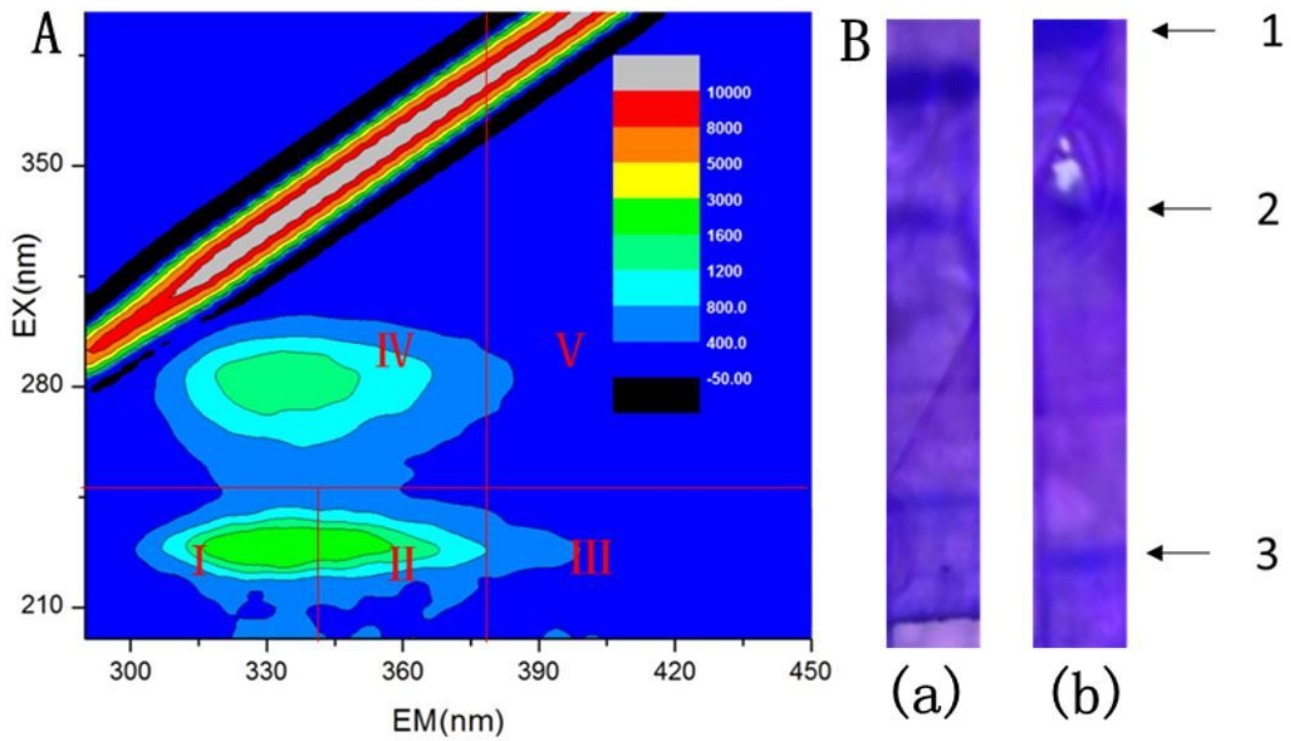


Figure 1

Three-dimensional excitation-emission-matrix (EEM) fluorescence (A) and Zymogram after SDS-PAGE of multi-enzymes visualized with ABTS (B). (a): multi-enzymes; (b): The following standards (Sigma) were used: bovine serum albumin (66 kDa), ovalbumin (45 kDa) and β -lactoglobulin (18.4 kDa). The standard protein bands were stained with Coomassie Blue R dye.

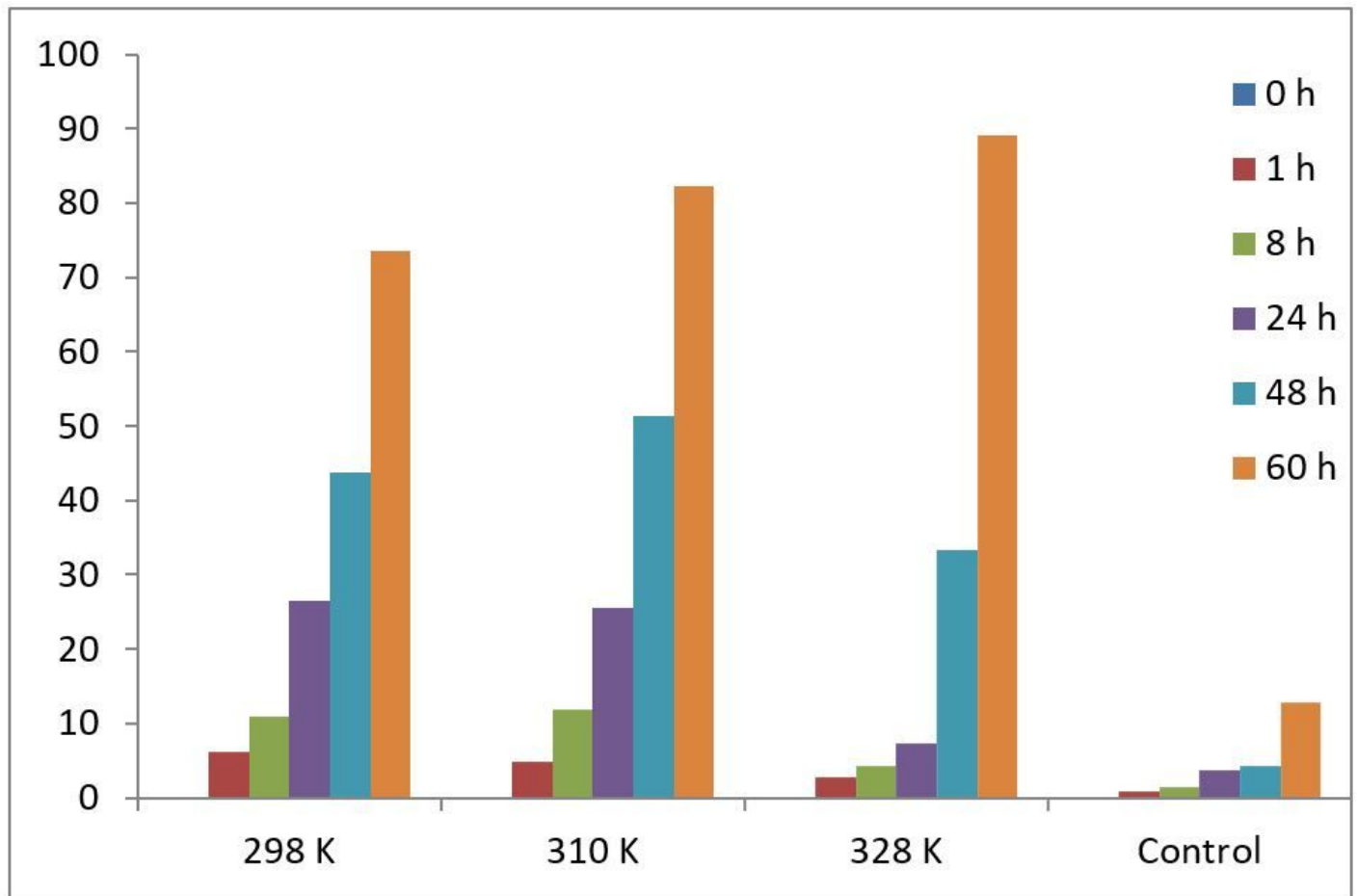


Figure 2

Removal of BPS by multi-enzymes. Conditions: C(multi-enzymes)= 75 mg/L, C(BPS)= 20 mg/L, pH = 7.4, T = 298 K, 310 K and 328 K.

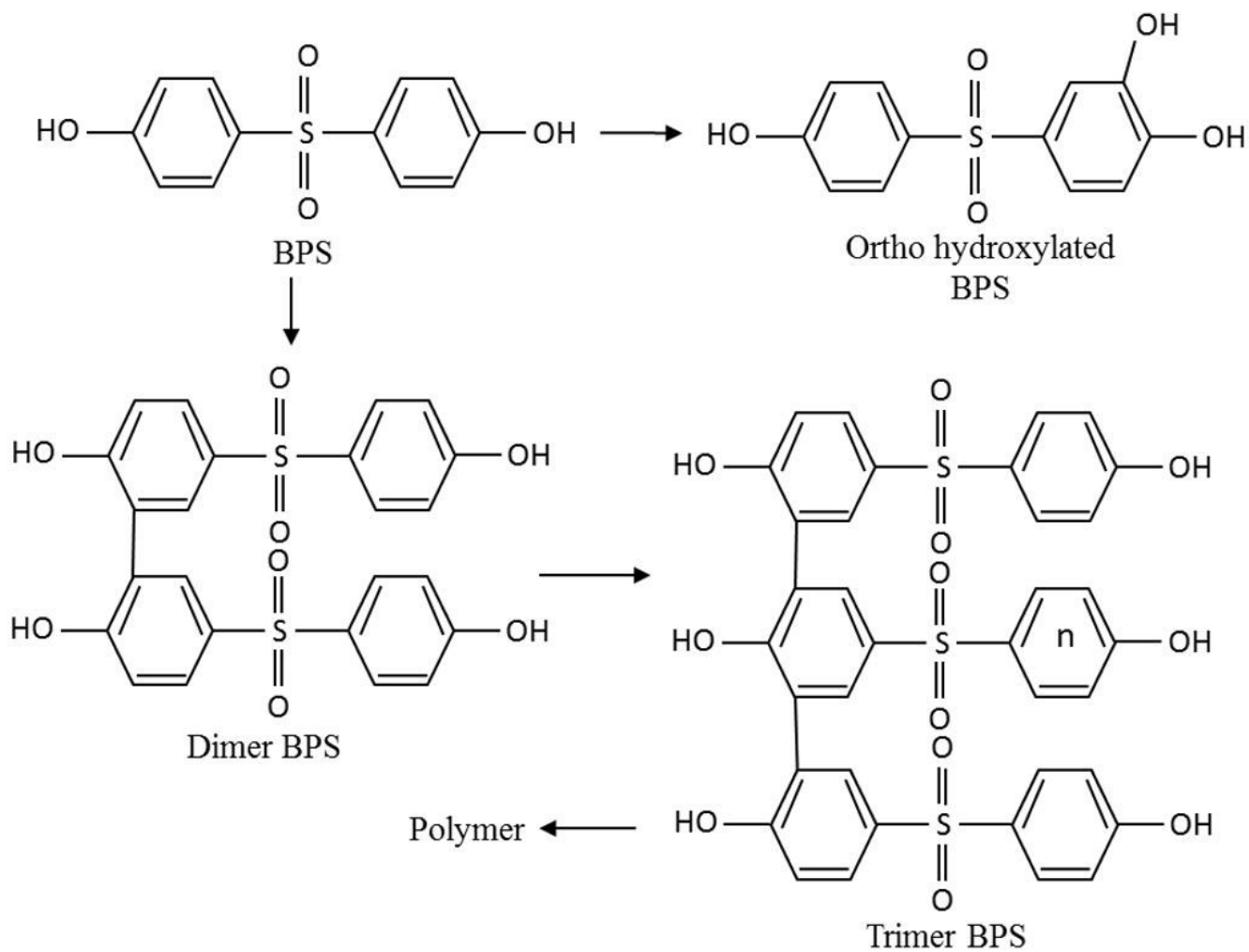


Figure 3

Proposed scheme of the BPS bio-transformation.

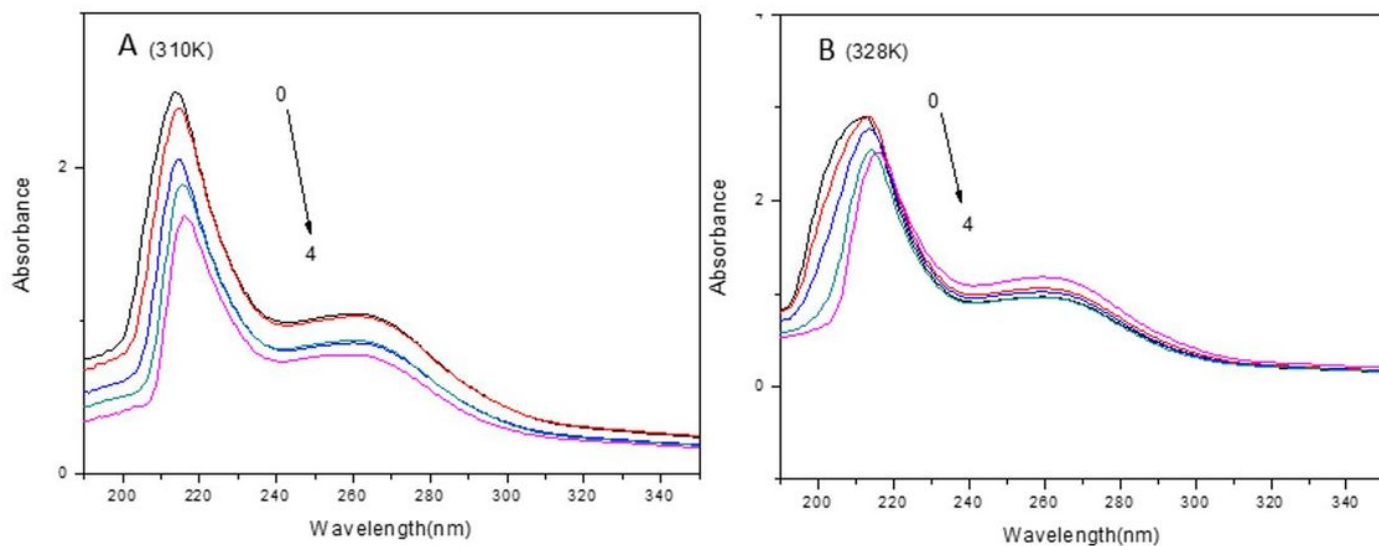


Figure 4

UV-vis absorption spectra of multi-enzyme with BPS. Conditions: C(multi-enzymes) = 75 mg/L, C(BPS) 0-4: 0, 3.2, 6.4, 12.8, 19.2 (mg/L), pH = 7.4, T = 310 K and 328 K.

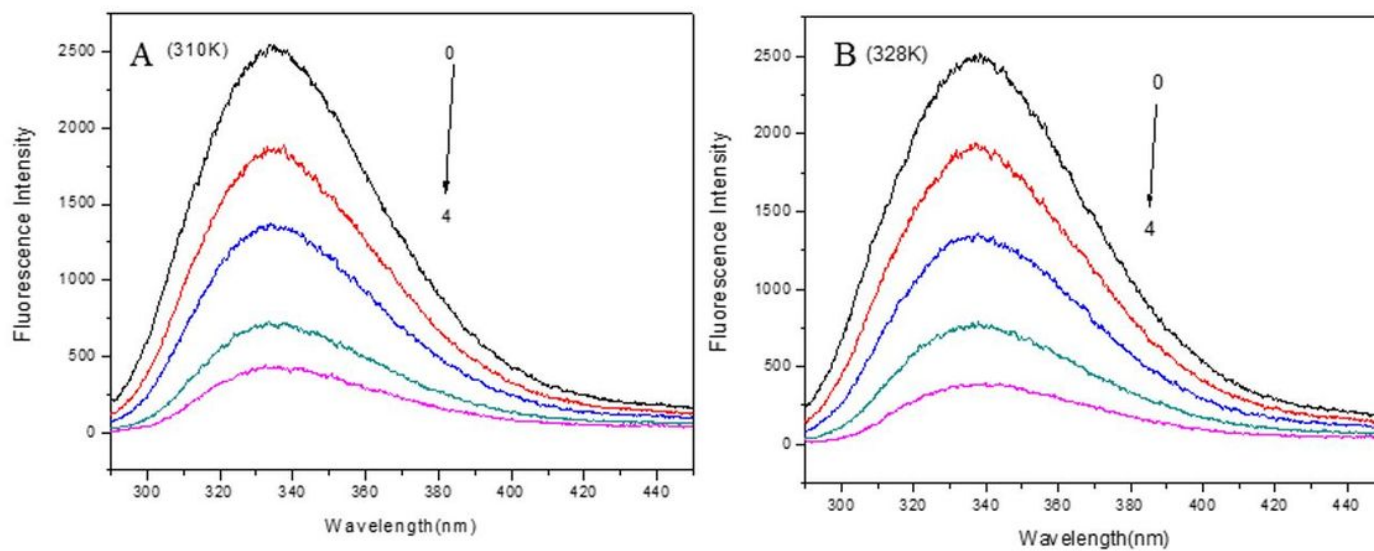


Figure 5

Fluorescence spectra of multi-enzyme in the presence of BPS. Conditions: C(multi-enzymes)= 75 mg/L, C(BPS) 0-4: 0, 3.2, 6.4, 12.8, 19.2 (mg/L), respectively; pH = 7.4; T = 310 K and 328 K.

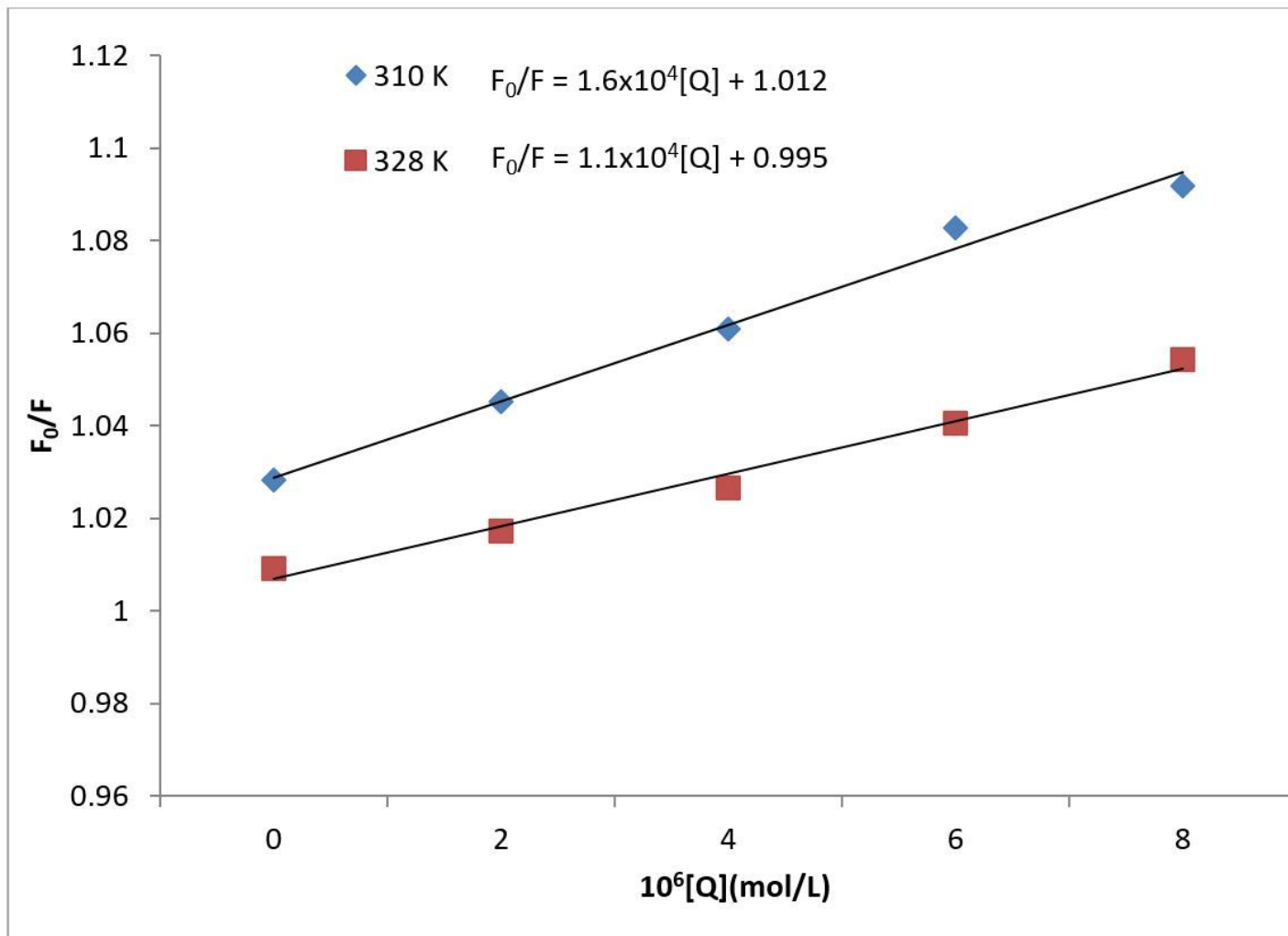


Figure 6

Stern–Volmer plots for the quenching of multi-enzyme. Conditions: C(multi-enzymes)= 75 mg/L, pH = 7.4; T = 310 K and 328 K.

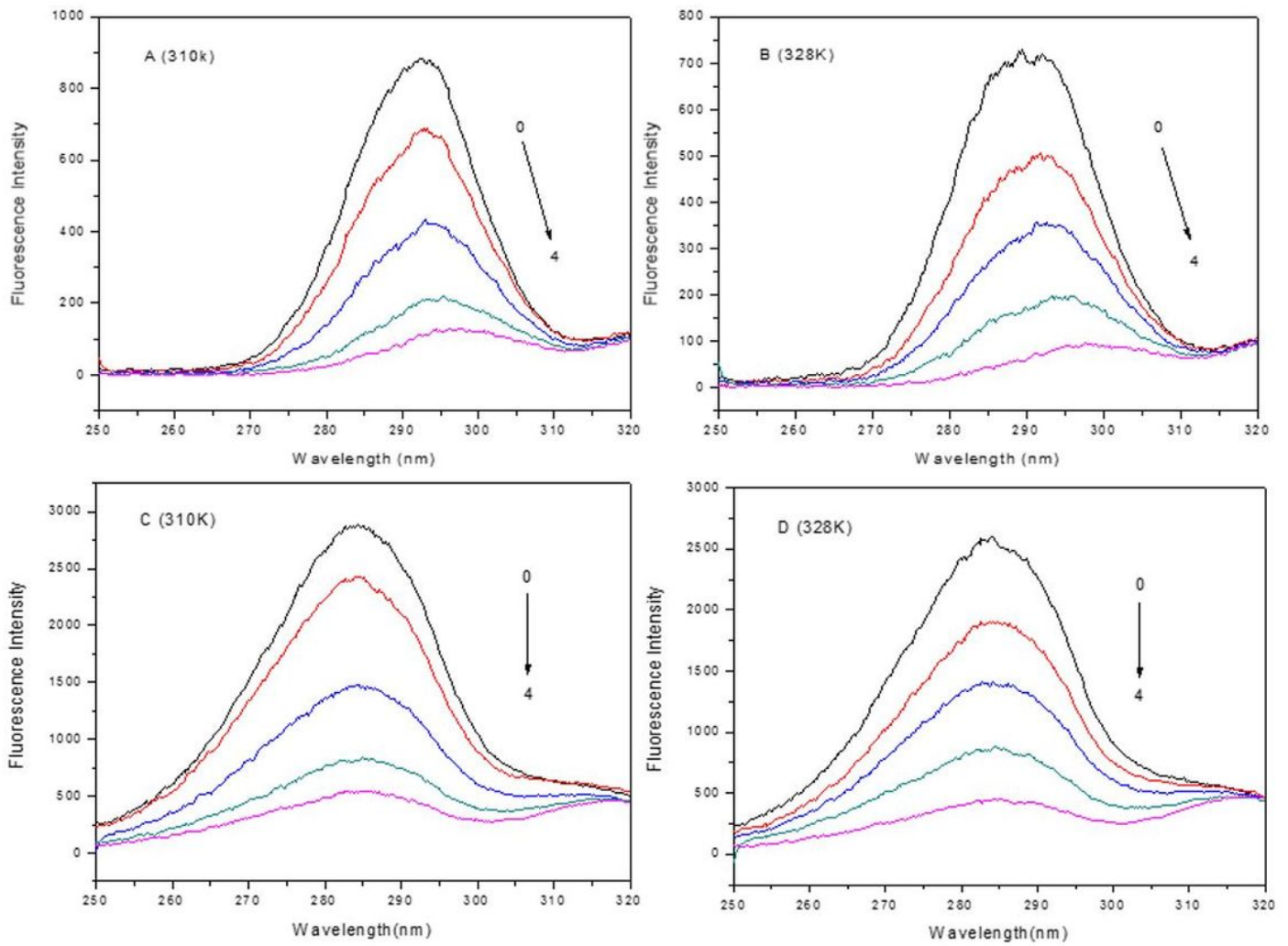


Figure 7

Synchronous fluorescence spectra ((A-B) $\Delta\lambda = 15$ nm and (C-D) $\Delta\lambda = 60$ nm) of multi-enzyme. Conditions: C(multi-enzymes)= 75 mg/L, C(BPS) 0-4: 0, 3.2, 6.4, 12.8, 19.2 mg/L), respectively; pH = 7.4.

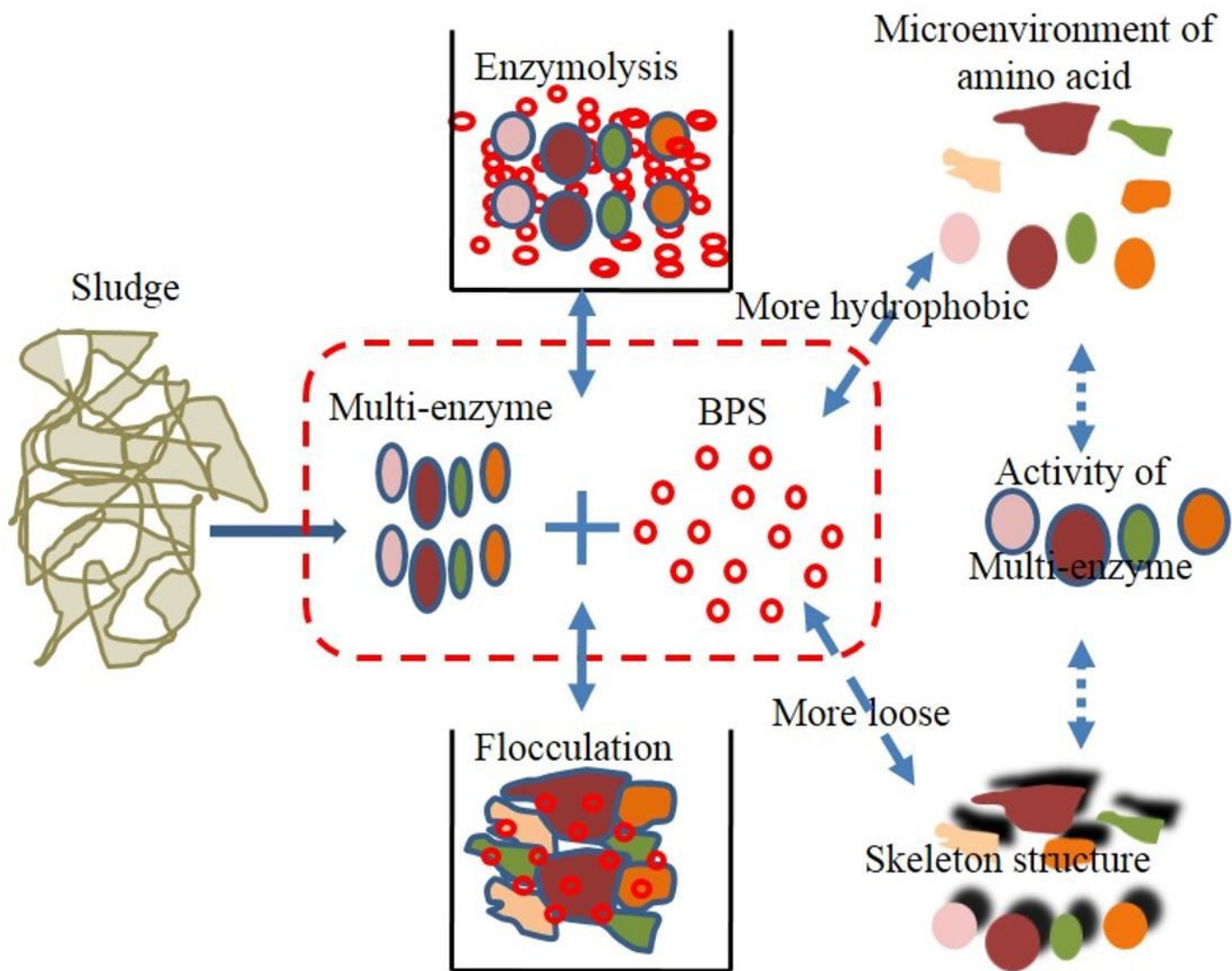


Figure 8

Visualized description of BPS removal by multi-enzyme and the interaction mechanism

Supplementary Files

This is a list of supplementary files associated with this preprint. Click to download.

- [Supportinformation.docx](#)